2007

Interfacial and Capillary Pressure Effects on the Thermal Performance of Wax/Foam Composites

Mohammad Rajab Almajali
University of Dayton

Khalid Lafdi
University of Dayton, klafdi1@udayton.edu

Shadab Shaikh
University of Dayton

Interfacial and capillary pressure effects on the thermal performance of wax/foam composites

M. Almajali,[a] K. Lafdi, and S. Shaikh
University of Dayton, 300 College Park, Dayton, Ohio 45469

(Received 30 March 2007; accepted 21 June 2007; published online 6 August 2007)

A numerical investigation study was performed to study the phase change behavior of wax/foam composite encapsulated in an aluminum casing. Two types of foam materials, namely, aluminum and carbon, were infiltrated with paraffin wax. The progress of melt interface and temperature distribution within the encapsulated composite was analyzed using computational fluid dynamics software (CFD). A two-energy equation model was implemented in the CFD software through the use of user defined function (UDF). Interfacial effects influencing the heat transfer process at the casing-composite junction and between the wax-foam surfaces within the composite were addressed through the use of separate UDF. In addition, the effect of capillary pressure developed within the foam matrix was incorporated using an area ratio parameter. The contact resistance at the foam-casing interface and the capillary pressure had a major influence on the thermal behavior of the system. These two factors lowered down the heat transfer rate considerably and the melting area was reduced by more than 30%. The temperature profiles for the foam material showed a different pattern as compared to the temperature within the wax, which was due to the effect of thermal nonequilibrium. © *2007 American Institute of Physics*. [DOI: 10.1063/1.2767268]

I. INTRODUCTION

Heat management is a critical issue in the design of modern electronic devices subjected to high heat densities and cyclic temperature variations. Among the different thermal management techniques the use of composite system with phase change material (PCM) impregnated within the foam matrix has gained increasing attention in recent times. Khateeb *et al.*[1,2] investigated the utilization of aluminum foams filled with paraffin wax (PCM) as a passive thermal management system for a lithium-ion battery. Py *et al.*,[3] Mills *et al.*,[4] and Zhang and Fang[5] investigated the enhancement of thermal conductivity of paraffin using a graphite matrix. The thermal conductivity of paraffin can be improved by impregnating porous graphite matrices with paraffin. However, the graphite matrix impregnated with paraffin can show considerable anisotropy with respect to the thermal conductivity.[4] Sari[6] investigated the preparation and thermal properties of paraffin/high density polyethylene (HDPE) composites as a thermal energy storage system. Mauran *et al.*[7] used a solid matrix made of graphite as a support for low thermal conductivity reactive salts. This support presented several advantages such as achieving a high external heat transfer coefficient, very low bulk density, good mechanical properties, and chemical inertness. Hong and Herling[8] analyzed the effects of geometric parameters of foam on the thermal performance of PCM/aluminum foam heat sinks. They concluded that the aluminum foams with larger surface area density utilized more latent heat within a given period of time which helped in improving the thermal performance of the heat sink.

Most of the works carried out to enhance the thermal conductivity of the PCMs by addition of some kind of high thermal conductivity additives or porous structures are mainly experimental. These studies are primarily concentrated on analyzing the enhancement in the effective thermal conductivity of the composite. They did not take into account the phase change process and the molten liquid flow motion into consideration. In addition, they did not study the parameters that affect the performance of such composites in thermal management applications. Weaver and Viskanta[9] performed numerical and experimental investigations for phase change of water in saturated porous media contained in various enclosures. Beckermann and Viskanta[10] also combined numerical and experimental works for solid/liquid phase change in porous media with natural convection in the molten region. Recently, Mesalhy *et al.*[11] carried out numerical and experimental studies to investigate the thermal characteristics of a cylindrical thermal protection system made of carbon foam matrix saturated with PCM. They used carbon foam matrices with different porosities and thermal properties. Their results illustrated that the stability of the thermal performance of composite matrix was dependent on the porosity of the foam and was better for higher porosity foams. Their study revealed that the thermal conductivity of the composite matrix acted sharply to increase or decrease its heat absorption rate.

The process of studying the thermal behavior of a system consisting of PCM and foam is very complicated. Due to the difference of the thermal properties of the foam and the PCM; the heat will diffuse in different speeds and the temperature of the PCM will be kept nearly constant during the phase change. This will generate a state of nonthermal equilibrium and heat exchange between the two phases. This can be accepted when the thermal properties of the two phases are close to one another. Some of the works in literature[9,10]

[a]Author to whom correspondence should be addressed; electronic mail: almajamr@notes.udayton.edu

considered local thermal equilibrium between the solid matrix and the PCM, and this was acceptable because in their case the thermal conductivity of porous matrix was low.

It was revealed from literature review that different works that considered local thermal nonequilibrium dealt with heat conduction and convection without phase change processes. One of the earliest studies for convection heat transfer in a packed bed considering local thermal nonequilibrium was carried out by Vafai and Sozen[12,13] They presented an analysis for the forced convective flow of a gas or liquid through a packed bed of spherical solid particles. Recently Calmidi and Mahajan[14] and Phanikumar and Mahajan[15] studied natural and forced convection inside high porosity metal foam using a two-energy equation model. It was shown that the deviation from local thermal equilibrium became significant for high values of Darcy and Rayleigh numbers. For conduction heat transfer in porous media, Quintard and Whitaker[16] carried out an extensive analysis to determine the conditions for local thermal equilibrium. They concluded that the deviation from local thermal equilibrium would be significant if there is a large difference between the physical properties of the fluid and solid phase. Mesalhy *et al.*[17] performed a numerical study to analyze the phase change process in a PCM/foam cylindrical composite. They used the volume averaged technique to solve the conservation equations of mass, momentum, and energy with phase change inside the porous matrix. The critical problem of local thermal nonequilibrium was addressed by using separate energy equations for the two phases.

In addition to the above issues an important aspect which has been ignored in most studies is the interaction between the PCM-foam surfaces within the matrix of foam structure. The infiltration process of the PCM inside the foam depends on the surface energy of PCM and the foam and the bore size of the foam. So, in most cases, if the pore is very small and the foam surface energy is too low compared to the molten PCM, some air gaps or pockets are expected to form between the PCM and the pore surface. This would cause thermal resistance between the high thermal conductivity phase and the PCM. At the same time the low wettability would reduce the amount of infiltrated PCM which affects the overall heat capacity of the system. The size and shape of these air-trapped pockets are expected to depend on the pore shape and the PCM-carbon wettability. The formation of these air gaps would develop a pressure. This pressure would try to push against the surface tension of the PCM. The difference between the pressure in the liquid PCM and the air gap is known as the capillary pressure. The contact area between the PCM and the foam, which affects the thermal performance of the system, would also be changed as the pressure varies.

The present study dealt with a study on the phase change process of the PCM/foam composite encapsulated within a metal casing. The motivation behind the design of such encapsulated composite was its applicability as a heat sink or a thermal energy storage system in thermal management problems. The presence of casing would make the study of the phase change process of PCM/foam composite even more complicated. In addition to the interfacial effects between the PCM and the foam, there would be an effect from the interfacial resistance between the foam and the casing material. Also when the casing is heated, a pressure would build up inside the composite system, which would have a greater influence on the capillary pressure. The current work had two major objectives. The first part focused on implementing a numerical procedure with two equation energy model for a PCM filled porous system through the use of a fast computing computational fluid dynamics (CFD) software. The second part concentrated on the study and analysis of the phase change process and thermal performance of the encapsulated PCM/carbon foam composite by considering the effects of capillary pressure buildup and thermal interface resistance within the system.

II. NUMERICAL PROCEDURE

As discussed before the implementation of numerical methods for PCM infiltrated foam systems is very rare. The complexity arises especially due to the big difference in the thermal conductivities of the PCM and foam materials leading to local thermal nonequilibrium. Use of separate energy equations for the PCM and foam phases is the solution adopted by some authors. For the present study we implemented the numerical technique for the phase change analysis of PCM/foam composite using a CFD software (FLUENT 6.3). The basic idea was to adopt a robust numerical procedure which can significantly reduce the computation time so that detailed parametric studies can be carried out in future as regard to different thermal management applications.

A. Governing equations

The numerical solution was set up on FLUENT 6.3 to solve the phase change transfer using the coupled continuity, momentum, and energy equations by considering Boussinesq approximation for buoyancy induced liquid phase flow. The enthalpy-porosity technique is used for modeling the solidification/melting process. In this technique, the melt interface is not tracked explicitly. Instead, a quantity called the liquid fraction, which indicates the fraction of the cell volume that is in liquid form, is associated with each cell in the domain. The liquid fraction is computed at each iteration based on an enthalpy balance.

Continuity equation,

$$\frac{\partial \rho}{\partial t} + \nabla \cdot (\rho \mathbf{v}) = 0. \tag{1}$$

Momentum equation,

$$\frac{\partial}{\partial t}(\rho \mathbf{v}) + \nabla \cdot (\rho \mathbf{v}\mathbf{v}) = \nabla \cdot (\bar{\bar{\tau}}) - \nabla p + \rho \mathbf{g} + S, \tag{2}$$

where $\mathbf{v}$ is the velocity component, $\bar{\bar{\tau}}$ is the stress tensor, ρ is the density, p is the static pressure, and S is the momentum source term. The stress tensor is given by

$$\bar{\bar{\tau}} = \mu \left[(\nabla \mathbf{v} + \nabla \mathbf{v}^T) - \frac{2}{3} \nabla \cdot \mathbf{v} I \right], \tag{3}$$

where ρ is the dynamic viscosity and I is the stress tensor.

The $\rho\mathbf{g}$ term represents the buoyancy term which according to the Boussinesq approximation is given by

$$\rho\mathbf{g} = \rho_0\beta(T - T_0)g, \tag{4}$$

where ρ_0 is the constant value of density, T_0 is the operating temperature, and β is the coefficient of thermal expansion for the PCM.

The energy transport equation is modified in porous media regions with modifications to the conduction flux and the transient terms only. In the porous medium, the conduction flux uses an effective conductivity and the transient term includes the thermal inertia of the solid region on the medium. The combined energy equation for solid and liquid phases is given by

$$\frac{\partial}{\partial t}[\gamma\rho_f E_f + (1-\gamma)\rho_s E_s] + \nabla\cdot[\mathbf{v}(\rho_f E_f + p)] = \nabla\cdot\left[k_{\text{eff}}\nabla T - \left(\sum_i h_i J_i\right) + (\bar{\bar{\tau}}\cdot\mathbf{v})\right] + S_f^h, \tag{5}$$

where E_f is the total fluid (PCM) energy, E_s is the total solid medium (porous matrix) energy, γ is the porosity of the medium, k_{eff} is the effective thermal conductivity, and S_f^h is the fluid enthalpy source term.

The energy equation given in Eq. (5) is used for both the porous matrix and the fluid inside it which, in this case, is the PCM. This is not considered as a favorable approximation when there is a big difference in thermal conductivity between the liquid and solid phases. Since there is huge difference in the thermal conductivity of PCM and the foam material which we have considered for the composite analysis, two separate energy equations were considered for the PCM and foam, respectively. In order to implement the two-energy equations in fluent, the concept of user defined scalar was used.

B. User defined energy equation

By using FLUENT it is possible to solve the transport equation for an arbitrary, user defined scalar (UDS) in the same way that it solves the transport equation for a scalar such as species mass fraction. Therefore, in order to implement the idea of two-energy equations considering local thermal nonequilibrium between two phases the combined energy equation (5) was divided into two parts. The default energy equation in FLUENT was solved for the PCM phase and the energy equation for the porous matrix was solved using the UDS. The interaction between the UDS energy equation and the default energy equation was achieved through the source terms. The separate energy equations used for the fluid (PCM) and solid (porous matrix) phases are given below.

PCM phase energy equation,

$$\frac{\partial}{\partial t}[(\gamma\rho_s C_{pf} T_f)] + \nabla\cdot(\rho_f C_{pf} T_f) = \nabla\cdot[(\alpha)k_{fe}\nabla T_f] + S_h + h_{sf}\left(\frac{A}{V}\right)(T_s - T_f). \tag{6}$$

Solid matrix energy equation,

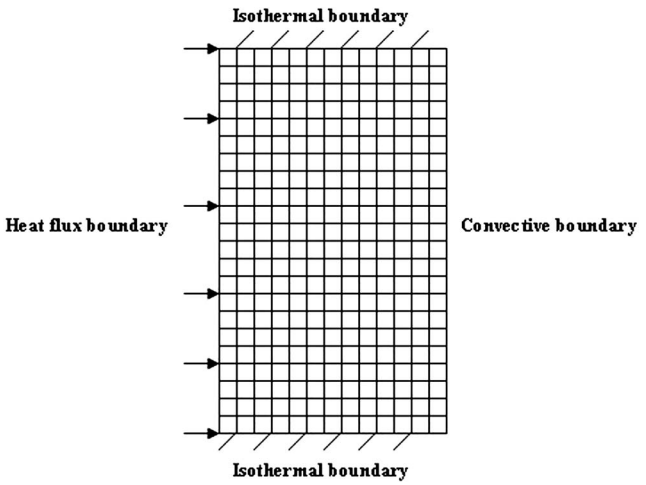

FIG. 1. Literature model for wax/foam composite.

$$\frac{\partial}{\partial t}\{[(1-\gamma)\rho_s C_{ps} T_s]\} = \nabla\cdot[(1-\alpha)k_{se}\nabla T_s] + h_{sf}\left(\frac{A}{V}\right)(T_f - T_s), \tag{7}$$

where S_h is the enthalpy source term, k_{fe} and k_{se} are the effective thermal conductivities of the fluid and solid phases, respectively, and the last term on right side of both equations represents the interfacial heat transfer with h_{sf} being the interfacial heat transfer coefficient.

C. Interfacial heat transfer

When applying the condition for local thermal nonequilibrium between the fluid and solid phases some important parameters need to be considered for the two-energy equation model. These parameters are the effective thermal conductivity for the two phases, the interfacial heat transfer coefficient, and the interfacial surface area. The effects of interfacial surface area are considered in later section. The equation for the interfacial heat transfer as shown in the PCM and foam energy equations (6) and (7) was used as the source term and implemented in FLUENT through a user defined function (UDF). The interfacial heat transfer coefficient was considered from the work of Lafdi *et al.*[18]

D. Validation of numerical technique

Before using the numerical procedure to analyze the phase change heat transfer in the encapsulated composite, it was validated by comparing with the experimental work of Lafdi *et al.*[19] for the phase change process of wax/aluminum foam composite. The modeling domain for this composite is shown in Fig. 1 below. The composite consists of aluminum foam infiltrated with paraffin wax. The left boundary of the composite is subjected to heat flux with the top and bottom surfaces being insulated. The right boundary is cooled by convective flow with cold water.

The numerical procedure was used to obtain the plots for the progress of the melt interface for phase change process of the wax/aluminum foam composite experimentally tested by Lafdi *et al.*[19] Figure 2 gives the plots for the comparison

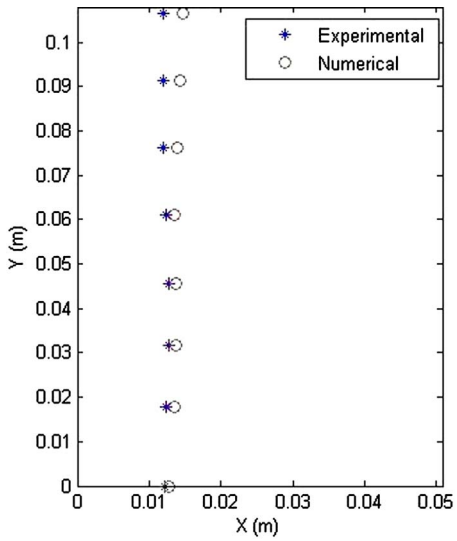

FIG. 2. (Color online) Comparison of melt interface for wax/foam composite with literature.

between the present work and the literature experimental results. It was observed that the results predicted by the numerical procedure are in a very good agreement with literature for all the time intervals. The slope of the melt interface from the top to the bottom shows a similar trend. The good agreement between the two results is supportive of the present numerical approach.

III. ANALYSIS FOR ENCAPSULATED COMPOSITE

A. Physical model

The modeling domain used for the encapsulated composite is shown in Fig. 3. The composite was made of a high thermal conductivity foam material saturated with PCM. A two dimensional model with a height of 5 cm and a width of 5 cm was considered for composite system. The PCM/foam composite was encapsulated in a thin casing with a thickness of 3.175 mm. The system was heated from left side subjected to an isothermal boundary condition above the melting temperature of PCM. The right wall was also kept at a constant

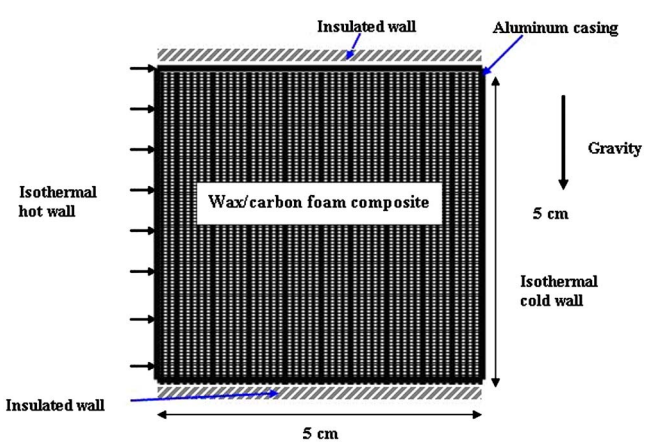

FIG. 3. (Color online) Model of the encapsulated PCM/foam composite inside aluminum casing.

TABLE I. Thermophysical properties of the PCM.

Property		Property	
T_m (K)	303	ρ (kg/m^3)	800
k (W/mK)	0.15–0.2	L (kJ/kg)	155–157
μ (kg/m s)	0.004 15	β (1/K)	0.000 85
c_p (J/kg K)	2460	σ (J/m^2)	0.023 65

temperature below the initial temperature of the system. The upper and lower surfaces of the system were considered as adiabatic boundary.

The PCM used for the study was a high latent heat paraffin wax. The thermo-physical properties of the paraffin wax (Table I) were taken from the work of Lafdi *et al.*[19] Two types of foam materials were considered for the analysis, namely, aluminum and carbon foams. The physical and thermal properties of the foam materials were also taken from the experimental work of Lafdi *et al.*[20] The aluminum foam used for the study had a porosity of 94% with 10 ppi pore size and effective thermal conductivity of 5.2 W/mK. The carbon foam used had a porosity of 94% with a relatively high effective thermal conductivity of 50 W/mK and surface energy of 0.0018 J/m2. The thin casing around the composite was considered to be made up of aluminum material.

B. Thermal interface resistance

In order to simulate the conditions for phase change process of encapsulated wax/foam composite similar to practical situations, the thermal resistance between the casing and foam material was estimated theoretically. The well known thermal resistance model of Savija *et al.*[21] was used to estimate the joint resistance. The thermal interface resistance, between any two solids, is a function of several geometric, physical, and thermal parameters such as surface roughness and waviness, surface microhardness, thermal conductivity of the contacting solids, properties of the interstitial materials, and the contact pressure. From Ref. 21 the joint thermal resistance R_j depends on the contact and gap components and can be calculated as follows:

$$\frac{1}{R_j} = \frac{1}{R_c} + \frac{1}{R_g}, \tag{8}$$

where R_c is the microcontact resistance and R_g is the gap resistance.

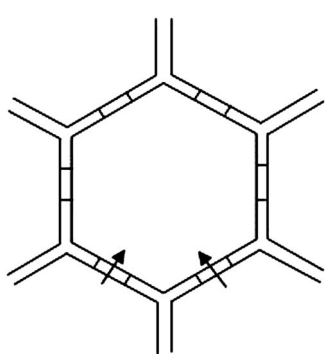

FIG. 4. Two dimensional (2D) representation for the pore.

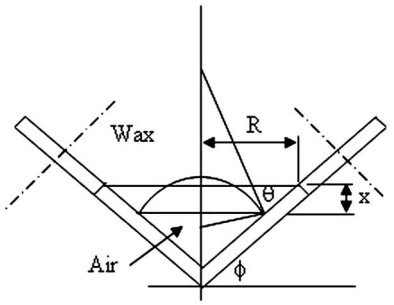

FIG. 5. Pore corner approximation.

The equation for joint resistance as obtained by Shaikh and Lafdi[22] can be calculated as

$$R_j = \left\{ \left[1.25K_s \left(\frac{m}{\sigma} \right) \left(\frac{P}{H_c} \right)^{0.95} + \frac{k_g}{Y+M} \right] A_a \right\}^{-1}, \tag{9}$$

where m is the effective absolute mean asperity slope, σ is the effective rms surface roughness of the two contacting surfaces, P is the contact pressure, Y is the layer thickness, H_c is the hardness of the material, k_g is the thermal conductivity of the layer, A_a is the apparent area of contact of two joining surfaces, and M is a coefficient and it is =0 if the gap is filled with thermal interface material, but if the gap is filled with air, $M=\alpha\beta\Lambda$, where the gas parameters $\alpha=2.4$, $\beta=1.7$, and molecular free path $\Lambda=0.06$ μm. This relation given by Eq. (9) was used to calculate the thermal contact resistance R_j at the interface between the composite and the casing.

C. Capillary pressure effects

As discussed before the process of PCM infiltration within the pores of the foam matrix can produce the capillary pressure. The capillary pressure would change the contact area between the PCM and the foam. The factors that have major effects on the capillary pressure are the surface energy of the foam and its pore size. Since the surface energy of aluminum is high and its pore size is also relatively high the effects of capillary pressure were neglected in the present study. However, the carbon foam pore size is very small and the surface energy of the untreated carbon is too low compared to the surface energy of molten PCM; hence the capillary pressure could have a significant impact on the heat transfer and phase change of the encapsulated composite.

In order to incorporate the effects of capillary pressure in the numerical technique implemented in FLUENT, a UDF was used. Lafdi *et al.*[23] had found a relationship for the area ratio, which is the ratio between the actual area of contact and the total contact area for liquid PCM within pores of foam matrix. This relation was obtained in terms of the capillary pressure and surface energy.

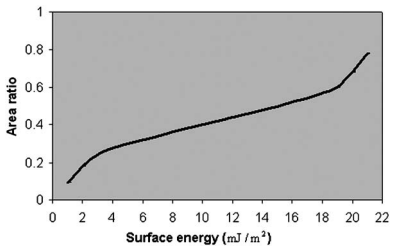

FIG. 6. Change of area ratio with carbon surface energy.

The pore of the carbon foam was approximated as a hexagon, as shown in Fig. 4. Since the corners of the pores would be the most probable spaces to entrap air, it was assumed that some air pockets would be formed in these corners and the surface tension force would try to push the PCM inside the corner against the trapped air pressure. The corner region was approximated as a conical shape with an angle ranging between 90° and 120°, and the open region in the ligament was assumed to be 1/3 of the ligament length, as shown from Fig. 5.

The capillary pressure was defined as

$$P_c = \frac{2\sigma_l \sin(\theta+\phi)}{R - x\cot\phi}, \tag{10}$$

where θ is the contact angle, σ_l is the surface tension of liquid PCM, ϕ is the corner angle, and R is the maximum radius of the groove.

The contact angle and the surface energy of each material were correlated as $\cos\theta = 2\sqrt{\sigma_s\sigma_l} - 1$, where σ_s is the surface energy of the foam. The gas inside the groove was assumed to obey the ideal gas law and was compressed isothermally, so the balance force between the liquid pressure and the capillary pressure with the compressed gas pressure inside the groove was written as

$$P_l + \frac{2\sigma_l \sin(\theta+\phi)}{R - x\cot\phi} = P_{\text{init}} \frac{V_{\text{init}}}{V}, \tag{11}$$

where P_{init} and V_{init} are the initial pressure and volume of the gas inside the groove. It was assumed that the initial volume of the gas was the total volume of the conical groove and the volume at equilibrium was calculated from the geometry in Fig. 5. Equation (12) will be rewritten as

$$1 + \frac{2\sigma_l}{RP_l} \frac{\sin[\pi - (\theta+\phi)]}{1 - (x/R)\cot\phi} = \frac{P_{\text{init}}/P_l}{[1 - (x/R)\cot\phi]^3} f(\theta,\phi), \tag{12}$$

where

$$f(\theta,\phi) = \frac{\tan\phi}{[2/\sin(\pi-\theta-\phi) + 1/\tan(\pi-\theta-\phi)][1/\sin(\pi-\theta-\phi) - 1/\tan(\pi-\theta-\phi)]^2 + \tan\phi}.$$

This above relation is a cubic equation, which was solved for $[1-(x/R)\cot\phi]$. Finally, the contact area between the carbon surface and the PCM for each corner was obtained as

$$A_{\text{cont}}/A_T = \sqrt{x^2 + x^2\cot^2\phi}(2R - x\cot\phi)/(R^2\sqrt{1+\tan^2\phi}). \quad (13)$$

Lafdi *et al.*[23] plotted the area ratio for different surface energies of the carbon foam (Fig. 6). It was observed that with the increase in surface energy of the carbon foam the area ratio also increases, indicating a better contact for the liquid PCM within the pores of the foam matrix. The area ratio can thus be used as a weighting factor for the interfacial heat transfer coefficient between the PCM phase and carbon foam material. The UDF file developed for the interfacial heat transfer within the foam matrix in the previous model was modified to include the area ratio to incorporate the effects of capillary pressure.

IV. RESULTS AND DISCUSSIONS

The numerical procedure thus developed was used for the phase change analysis of the encapsulated composite by considering the various effects due to interfacial heat transfer within the composite matrix, thermal resistance between the foam and casing, and the capillary pressure within the porous matrix. The numerical technique was implemented stepwise to study the influence of each factor.

A. Effect of interfacial heat transfer

For the first case only the thermal resistance at foam-casing interface and the capillary pressure was neglected. A comparison was made for the phase change heat transfer of encapsulated composite only for effects of interfacial heat transfer within the composite matrix. Numerical simulations were carried out for 45 min for approximately 60% melting of the encapsulated composite first without any interfacial heat transfer then with interfacial heat transfer through the UDF. Figure 7 shows the melt interface after time intervals of 30 and 45 min for both situations.

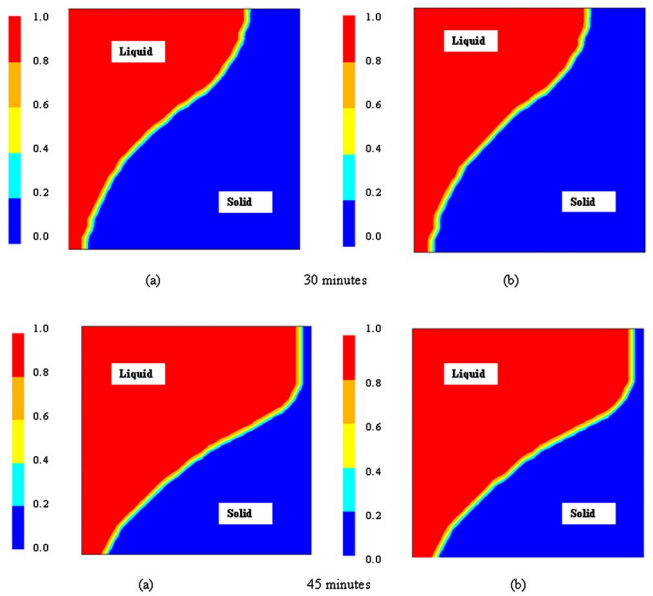

FIG. 7. (Color online) Melt interface for encapsulated composite: (a) without interfacial effect and (b) with interfacial effect.

It was observed that with the inclusion of interfacial heat transfer effect within the composite matrix melting rate was reduced. The melted area with interfacial heat transfer was 4.96% less as compared with the case when the interfacial effects were neglected. This could be due to the thermal resistance within the pores at the foam-wax interfaces. Figure 8 gives the plot for the temperature profiles with the carbon foam and paraffin wax corresponding to a melting duration of 30 min. The two-energy equation model implemented through the UDS was used to obtain the temperature distributions for the carbon foam and wax materials. The effect of thermal nonequilibrium is clearly visible in Fig. 8 with the temperature profiles for the wax differing from that of the carbon foam.

B. Effect of casing-foam thermal resistance

Figure 9 shows the temperature contours for the wax and carbon foam (30 min melting) after the contact resistance

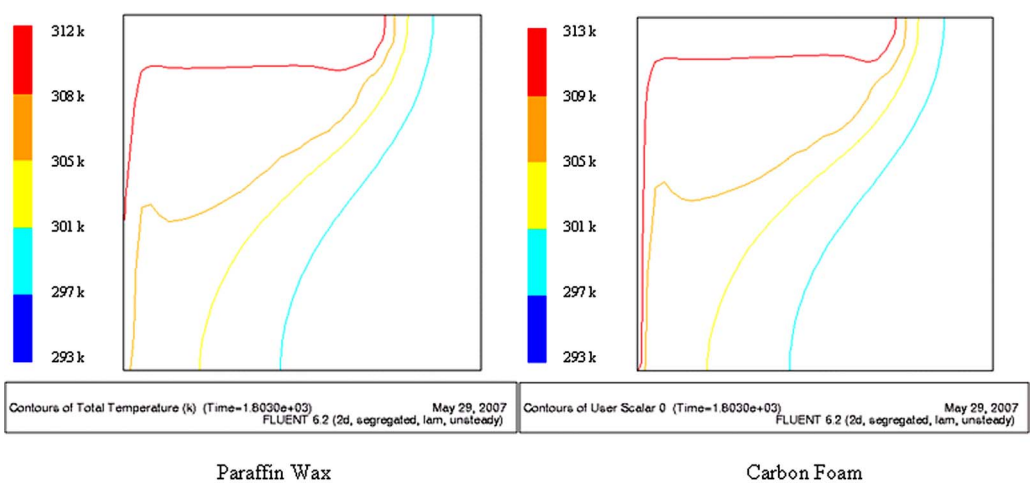

FIG. 8. (Color online) Temperature profile for encapsulated composite with interfacial heat transfer effects: (a) paraffin wax and (b) carbon foam.

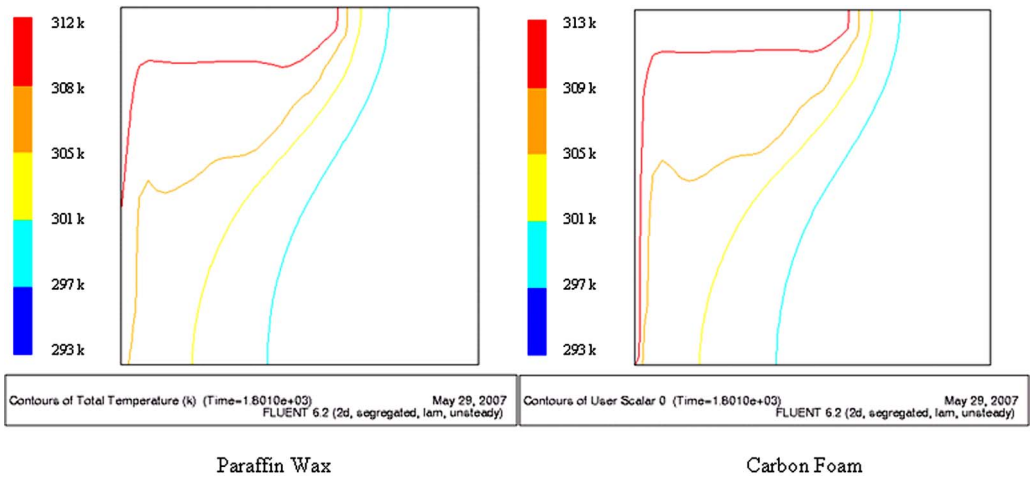

FIG. 9. (Color online) Temperature profile for encapsulated composite with casing-foam thermal resistance: (a) paraffin wax and (b) carbon foam.

between the casing-foam interfaces was included. There is a difference in pattern for temperature distribution for the two materials due to thermal nonequilibrium. The heat propagation was faster through carbon foam as compared to the wax. The melting area was reduced by 16%, as shown in Fig. 10(a) for both melting times of 30 and 45 min when compared to the case in Fig. 8(a). This was due to the thermal resistance at the casing-foam interface which caused a significant drop in heat transfer between the casing and the foam composite. Thus the effect of thermal interface resistance can have a considerable impact on the overall phase change heat transfer of the encapsulated heat and its effect cannot be neglected.

C. Effect of capillary pressure

For the final case the effect of the capillary pressure was included by modifying the UDF used implemented for the interfacial heat transfer within foam/wax composite. Figure 10(b) shows the progress of melt interface after 30 and 45 min for this case as compared to the case without capillary pressure [Fig. 10(a)]. It was observed that the melting rate considerably reduced with the inclusion of capillary pressure. The melted area for Fig. 10(b) was 15% less as compared to Fig. 10(a). This was expected since the capillary pressure resulted in the formation of air pockets, which caused a reduction in the contact area for the liquid wax within the foam pores. On the other hand when the effects of capillary pressure were neglected a perfect contact between wax and foam was assumed. Figure 11 gives the temperature profiles for the wax and foam materials (30 min) for the capillary pressure case. It is clear from this figure that the heat propagation is slower for both wax and the carbon foam for this case as compared to Fig. 9, due to the reduction in melting rate.

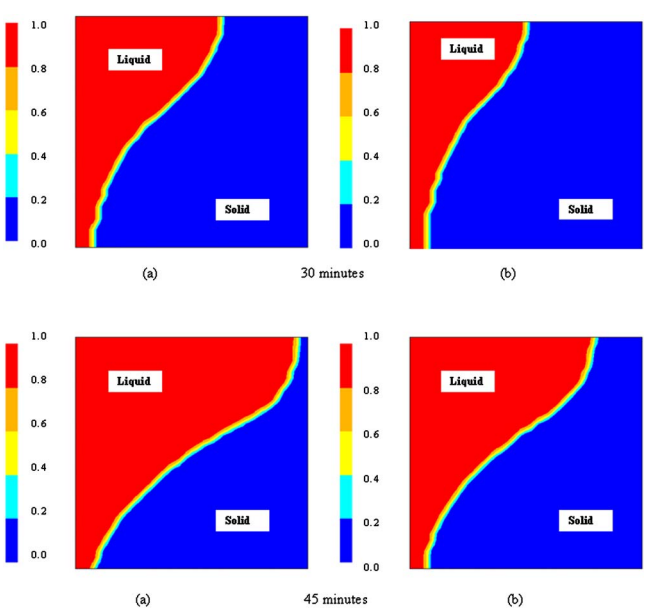

FIG. 10. (Color online) Melt interface for encapsulated composite: (a) without capillary pressure and (b) with capillary pressure.

V. CONCLUSIONS

A numerical technique was implemented using CFD software to study the phase change process within an encapsulated wax/foam composite. The numerical procedure for the wax infiltrated porous foam was solved using a two-energy model to tackle the problem of local thermal nonequilibrium. Three important factors affecting the heat transfer process of encapsulated composite were considered in the study. Interfacial effects influencing the heat transfer process at the casing-composite junction and between the wax-foam surfaces within the composite were addressed through the use of UDF. In addition to this, the effect of capillary pressure developed within the foam matrix and its impact on the heat transfer process was incorporated using an area ratio parameter. The numerical method was first compared with an experimental study from literature for the phase change process of wax/aluminum foam composite. An excellent agreement was found between both results. A stepwise analysis was then carried out for the encapsulated wax/carbon foam composite by considering the effects of different factors. For each case the encapsulated composite was analyzed for a melting time of 30 min. The interfacial heat transfer within the foam composite and the thermal resistance at the casing-foam interface caused a considerable reduction in the melt-

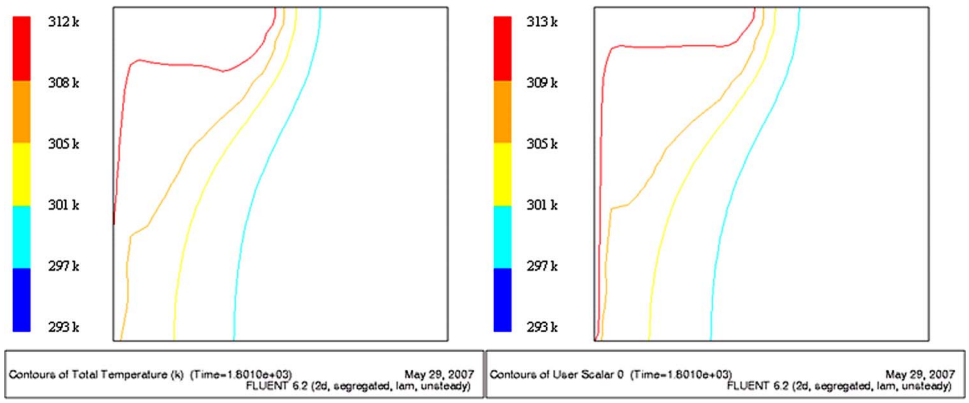

FIG. 11. (Color online) Temperature profile for encapsulated composite with capillary pressure: (a) paraffin wax and (b) carbon foam.

ing rate and the melted area was reduced by 16% with these effects included. The inclusion of capillary pressure further lowered down the melting rate and an overall reduction of more than 30% was observed in the melted area. The temperature distribution for all the cases showed a deviation for the wax and carbon foam materials due to the presence of thermal non-equilibrium. The current study revealed the impact of the interfacial heat transfer within composite, thermal contact resistance, and the capillary pressure within the pores of the foam matrix on the overall phase change process of the encapsulated composite. The present work will be extended in future to carry out a detailed parametric study to analyze the effects of the above factors for different foam materials and ways to minimize the effects of these factors on the heat transfer process.

[1]S. A. Khateeb, M. M. Farid, J. R. Selman, and S. Al-Hallaj, J. Power Sources **128**, 292 (2004).
[2]S. A. Khateeb, S. Amiruddin, M. Farid, J. R. Selman, and S. Al-Hallaj, J. Power Sources **142**, 345 (2005).
[3]X. Py, R. Olives, and S. Mauran, Int. J. Heat Mass Transfer **44**, 2727 (2001).
[4]A. Mills, M. Farid, J. R. Selman, and S. Al-Hallaj, Appl. Therm. Eng. **26**, 128 (2006).
[5]Z. Zhang and X. Fang, Energy Convers. Manage. **47**, 303 (2006).
[6]A. Sari, Energy Convers. Manage. **45**, 2033 (2004).
[7]S. Mauran, P. Prades, and F. L'haridon, Heat Recovery Syst. CHP **13**(4), 315 (1993).
[8]S. T. Hong and D. R. Herling, Scr. Mater. **55**, 887 (2006).
[9]J. A. Weaver and R. Viskanta, Int. Commun. Heat Mass Transfer **13**(3), 245 (1986).
[10]C. Beckermann and R. Viskanta, Int. J. Heat Mass Transfer **31**, 35 (1988).
[11]O. Mesalhy, K. Lafdi, and A. Elgafy, Carbon **44**, 2080 (2006).
[12]K. Vafai and M. Sozen, ASME J. Heat Transfer **112**, 690 (1990).
[13]K. Vafai and M. Sozen, ASME J. Heat Transfer **112**, 1014 (1990).
[14]V. V. Calmidi and R. L. Mahajan, ASME J. Heat Transfer **121**, 466 (1999).
[15]M. Phanikumar and R. Mahajan, Int. J. Heat Mass Transfer **45**, 3781 (2002).
[16]M. Quintard and S. Whitaker, Adv. Heat Transfer **23**, 369 (2003).
[17]O. Mesalhy, K. Lafdi, and A. Elgafy, Energy Convers. Manage. **46**, 847 (2005).
[18]K. Lafdi, O. Mesalhy, K. Lafdi, and S. Shaikh, Appl. Phys. A: Mater. Sci. Process. (submitted).
[19]K. Lafdi, O. Mesalhy, and S. Shaikh, Energy Convers. Manage. (submitted).
[20]K. Lafdi, O. Mesalhy, and S. Shaikh, Energy Convers. Manage. (submitted).
[21]I. Savija, J. R. Culham, M. M. Yovanovich, and E. E. Marotta, 40th AIAA Aerospace Sciences Meeting and Exhibit (AIAA-2002-0494), Vol. 17, (Reno, NV, 2002), pp. 43–52.
[22]S. Shaikh and K. Lafdi, Carbon **45**, 695 (2007).
[23]K. Lafdi, O. Mesalhy, and S. Shaikh, Carbon (in press).